Decays of B_s^0 Mesons and b Baryons: A Review of Recent First Observations and Branching Fractions

Andreas Warburton
(on behalf of the Belle, CDF, and DZero Collaborations)

McGill University, Montréal, Québec, Canada

Recent rate measurements of B_s^0 mesons and Λ_b^0 baryons produced in $\sqrt{s} = 1.96$ TeV proton-antiproton and $\Upsilon(5S)$ electron-positron collisions are reviewed, including the first observations of six new decay modes: $B_s^0 \to D_s^+ K^-$ (CDF), $B_s^0 \to D_s^- D_s^+$ (CDF), $B_s^0 \to D_{s1}^-(2536)\,\mu^+\,\nu_\mu\,X$ (DZero), $B_s^0 \to \phi\,\gamma$ (Belle), $\Lambda_b^0 \to p\,\pi^-$ (CDF), and $\Lambda_b^0 \to p\,K^-$ (CDF). Also examined are branching-fraction measurements or limits for the $B_s^0 \to D_s^{(*)}\,D_s^{(*)}$ modes (Belle, CDF, and DZero), the $B_s^0 \to \gamma\,\gamma$ radiative penguin decay (Belle), and three two-body charmless B_s^0 meson decay channels (CDF). Implications for the phenomenology of electroweak and QCD physics, as well as searches for physics beyond the Standard Model, are identified where applicable.

1. Introduction

Heavier b-flavoured hadrons represent a fecund source of particle physics. While the rich interplay between electroweak and non-perturbative strong effects typically poses formidable experimental and theoretical challenges, decays of hadrons with masses at the frontiers of Standard Model spectroscopy constitute an exciting proving ground for effective theories, QCD factorization and lattice methods, as well as potential models. Moreover, such heavy hadronic states present opportunities to uncover real or constrain hypothetical new physics lying beyond the Standard Model.

The measurement of observables from b baryons and strange or charmed B mesons is complementary to the wealth of physics that the BABAR, Belle, and CLEO collaborations have harvested from e^+e^- colliders operating at the $\Upsilon(4S)$ open-beauty threshold. Comparisons of heavy b-hadron decays to the analogous non-strange $B_{u,d}$ ($B^{+,0}$) decays can yield advantages that include cancellations of hadronic uncertainties, tests of $SU(3)$ flavour symmetry, decay-amplitude disentanglement, and improved access to fundamental electroweak parameters of Nature.

This paper reviews recent rate measurements of B_s^0 mesons and Λ_b^0 baryons produced in $\sqrt{s} = 1.96$ TeV proton-antiproton and $\Upsilon(5S)$ electron-positron collisions at the Fermilab Tevatron (USA) and KEKB (Japan) accelerator facilities, respectively. Described are first observations of $B_s^0 \to D_s^+ K^-$ and $B_s^0 \to D_s^- D_s^+$ decays[1] by CDF; recent results on $B_s^0 \to D_s^{(*)}\,D_s^{(*)}$ decays and worldwide status from Belle, CDF, and DZero; the first observation of $B_s^0 \to D_{s1}^-(2536)\,\mu^+\,\nu_\mu\,X$ by DZero; the first observation of the $B_s^0 \to \phi\,\gamma$ mode and a search for $B_s^0 \to \gamma\,\gamma$ decays by Belle; three recently updated measurements of charmless two-body B_s^0 meson decays by CDF; and first observations of $\Lambda_b^0 \to p\,K^-$ and $\Lambda_b^0 \to p\,\pi^-$ decays by CDF.

[1] Charge conjugate decays are implied throughout.

2. First $B_s^0 \to D_s^+ K^-$ Observation

The Cabibbo-suppressed $B_s^0 \to D_s^+ K^-$ mode, as indicated in Fig. 1, has contributions from both upper- and lower-vertex charm such that the same B_s^0 parent state can decay both to $D_s^+ K^-$ and $D_s^- K^+$ final states, as distinct from the analogous $B^0 \to D^- K^+$ mode. Due to the fact that these decay amplitudes can interfere through B_s mixing, the branching fraction relative to that of the Cabibbo-favoured reference mode, $\mathcal{B}(B_s^0 \to D_s^+ K^-)/\mathcal{B}(B_s^0 \to D_s^- \pi^+)$, can deviate significantly higher or lower than the analogous ratio of non-strange branching fractions, $\mathcal{B}(B^0 \to D^- K^+)/\mathcal{B}(B^0 \to D^- \pi^+)$. As is also evident from Fig. 1, the relative weak phase between the two final charge states is the angle γ (ϕ_3) of the CKM unitarity triangle, meaning that a flavour-tagged time-dependent analysis of $B_s^0 \to D_s^+ K^-$ could yield a theoretically clean [1] measurement of γ (ϕ_3). The possibility of an untagged approach relying on a significant lifetime difference between the B_s CP eigenstates has also been posited [2].

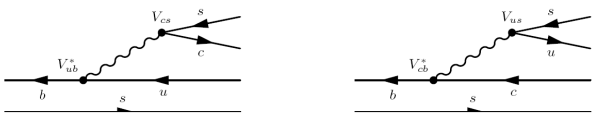

Figure 1: Upper- and lower-vertex charm diagrams contributing to $B_s^0 \to D_s^+ K^-$ decay [3].

The CDF collaboration recently reported [3] the first observation of $B_s^0 \to D_s^+ K^-$ decays and the first measurement of the $\mathcal{B}(B_s^0 \to D_s^+ K^-)/\mathcal{B}(B_s^0 \to D_s^- \pi^+)$ branching-fraction ratio using $D_s^- \to \phi\,\pi^-$ decays in 1.2 fb^{-1} of $p\bar{p}$ collisions at $\sqrt{s} = 1.96$ TeV. The

analysis made profitable use of CDF's Level 2 Silicon Vertex 2-Track Trigger [4], which could identify vertices from track pairs with significant impact parameters (between 0.12 and 1 mm), and therefore functioned as a valuable online means to identify relatively pure samples of hadronically decaying heavy-flavour hadrons. Two separate control samples were studied simultaneously to form analogous $D^{*-}\,K^+/D^{*-}\,\pi^+$ and $D^-\,K^+/D^-\,\pi^+$ ratios as cross checks. The selection criteria [3] involved no explicit particle identification requirements such that tracks were taken to be either kaons or pions to match the reconstruction hypothesis.

The principal challenge in this analysis was the disentanglement, using a multivariate maximum-likelihood fit, of the numerous components entering the $D_s^-\,\pi^+$ data sample. A simultaneous fit was performed in terms of the $D_s^-\,\pi^+$ invariant mass and a particle-identification variable Z describing the non-D_s^- daughter track, where $Z \equiv \log\left[dE/dx(\text{measured})/dE/dx(\text{expected for }\pi)\right]$ such that it is normally distributed. Mass templates were created from sizeable Monte Carlo samples to be used as probability density functions (PDFs) in the fit. Combinatorial background due to real D mesons was estimated using wrong-sign data, and the dE/dx Z-variable templates were derived largely from inclusive D^* data.

The fit, for which care was taken to treat the $D\,\pi$ radiative tail as a free parameter and correlations amongst the fit parameters were taken into account, identified 109 ± 19 $D_s\,K$ signal candidates with a statistical significance of 7.9 standard deviations. Invariant mass and Z projections from the likelihood fit are indicated in Figs. 2 and 3, respectively.

The resulting ratio of branching fractions was measured to be

$$\frac{\mathcal{B}(B_s^0 \to D_s^+\,K^-)}{\mathcal{B}(B_s^0 \to D_s^-\,\pi^+)} = 0.107 \pm 0.019(\text{stat.}) \pm 0.008(\text{syst.}), \tag{1}$$

for which the largest source of systematic uncertainty arose from the treatment of the Z variable templates. The result expressed in Eqn. 1 is statistically compatible with the analogous B^0 branching-fraction ratio, indicating that interference effects are not yet observable. A recent CDF measurement [5] also exists for the branching fraction of the normalization mode, $\mathcal{B}(B_s^0 \to D_s^-\,\pi^+)$, and may be used to extract an absolute branching fraction for $B_s^0 \to D_s^+\,K^-$ decays.

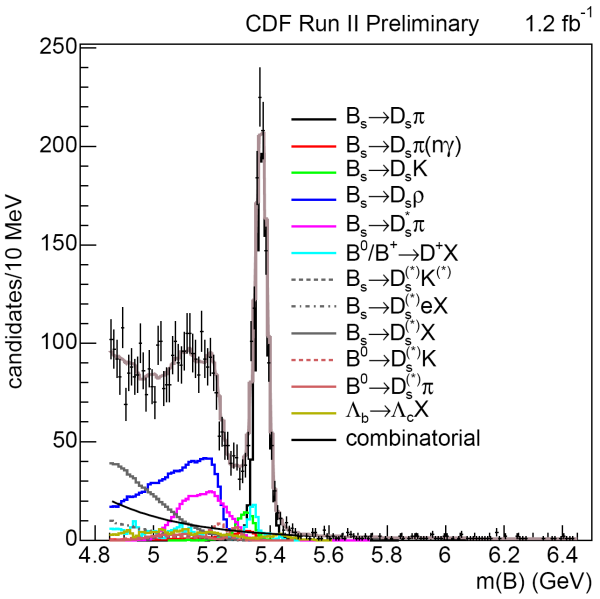

Figure 2: Invariant mass projections of the likelihood fit results for $B_s^0 \to D_s^-\,\pi^+$ candidates [3]. The fit result for the signal $B_s^0 \to D_s^+\,K^-$ distribution is indicated by the green histogram.

3. Recent $B_s^0 \to D_s^{(*)}\,D_s^{(*)}$ Decay Results

The suite of B_s^0 decays denoted by $B_s^0 \to D_s^{(*)}\,D_s^{(*)}$, representing the three decay modes $B_s^0 \to D_s^{*+}\,D_s^{*-}$, $B_s^0 \to D_s^{*+}\,D_s^-$, and $B_s^0 \to D_s^+\,D_s^-$, is considered to be the principal contributor to the rate difference $\Delta\Gamma_s^{CP}$ between the odd and even B_s^0 CP eigenstates. Mixing in the B_s^0 system has recently been observed, thus providing a precise measurement of the mass difference of the B_s^0 mass eigenstates [6]. To a good approximation, the mass eigenstates are expected to be eigenstates of CP such that their rate difference is equivalent to $\Delta\Gamma_s^{CP}$. Assuming $B_s^0 \to D_s^{(*)}\,D_s^{(*)}$ decays dominate the $b \to c\bar{c}s$ quark-level transitions, which are purely CP-even, the branching fraction is related to $\Delta\Gamma_s^{CP}$ by $\mathcal{B}(B_s^0 \to D_s^{(*)}\,D_s^{(*)}) = \Delta\Gamma_s^{CP}/2\Gamma_s$ in the Standard Model [7], which regards the CP-violating mixing phase as negligible. Studies of $\mathcal{B}(B_s^0 \to D_s^{(*)}\,D_s^{(*)})$, modulo theoretical assumptions about dominant CP content, can therefore reveal departures from the Standard Model in the form of new physics that renders the CP-violating mixing phase non-zero.

Although the overall $B_s^0 \to D_s^{(*)}\,D_s^{(*)}$ rates are expected to be large, studies of these modes are experimentally challenging due to the small fully hadronic charm-meson branching fractions. Two recent studies at the Tevatron are reviewed here, followed by a brief summary of the worldwide status of $B_s^0 \to D_s^{(*)}\,D_s^{(*)}$ decay measurements.

3.1. DZero Inclusive $\mathcal{B}(B_s^0 \to D_s^{(*)}\,D_s^{(*)})$

The DZero collaboration recently presented a preliminary inclusive measurement of $\mathcal{B}(B_s^0 \to D_s^{(*)}\,D_s^{(*)})$ based on a 2.8 fb^{-1} sample of $p\bar{p}$ collisions at $\sqrt{s} =$

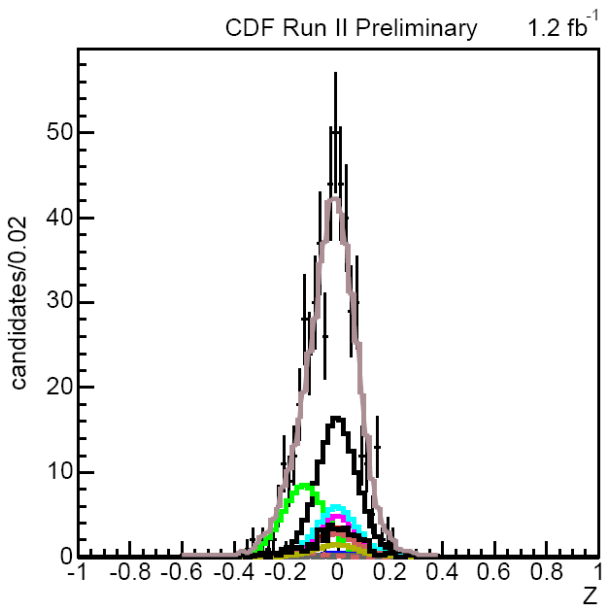

Figure 3: Z particle-identification projections of the likelihood fit results for $B_s^0 \to D_s^- \pi^+$ candidates for the $D_s \pi$ mass window corresponding to the $D_s K$ signal region ($5.26 - 5.35$ GeV/c^2) [3]. The colour coding is identical to that shown in Fig. 2, and the signal $B_s^0 \to D_s^+ K^-$ distribution is again shown in green.

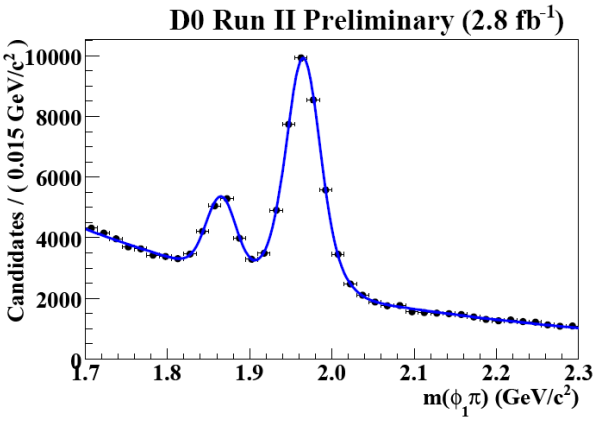

Figure 4: Inclusive $D^{(*)}$ candidate reconstruction in the μ sample, represented by the $\phi_1 \pi$ invariant mass distribution corresponding to the $K^+ K^-$ signal region, $1.01 < m(K^+ K^-) < 1.03$ GeV/c^2 [8]. The two peaks represent the observed $D^{\pm}$ and $D_s^{\pm}$ inclusive candidate yields.

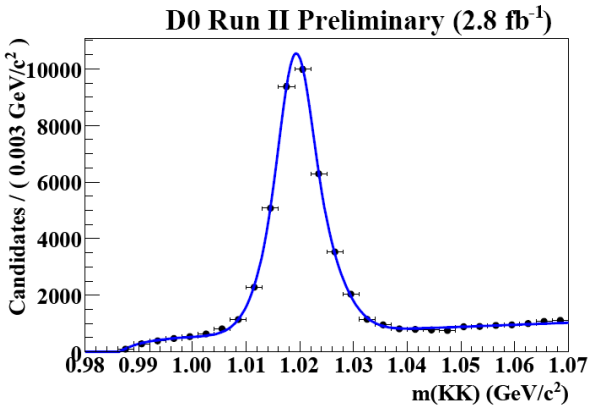

Figure 5: Inclusive $K^+ K^-$ invariant mass distribution for ϕ_1 candidates corresponding to the $\phi_1 \pi$ signal region, $1.92 < m(\phi_1 \pi) < 2.00$ GeV/c^2 [8].

1.96 TeV [8]. No distinction was made between the orbitally excited and ground-state $D_s^{(*)}$ mesons; the analysis therefore sought to identify correlations between final-state particles in a pair of candidate $D_s^{(*)}$ decays, the first involving a $\phi_1 \pi$ final state and the second involving a $\phi_2 \mu \nu$ final state, where ϕ_1 and ϕ_2 denote two mutually exclusive $\phi \to K^+ K^-$ candidate reconstructions in the same event. The majority of candidate events was collected using single-muon triggers by selecting a common sample [8] containing muon track candidates and $D_s \to \phi_1 \pi$ candidates.

A binned likelihood fit identified the inclusive number of $D_s \mu$ candidates as $28\,680 \pm 288$(stat.), taking into account possible $D^{\pm}$ contributions and combinatorial backgrounds. Figs. 4 and 5 illustrate the invariant mass distributions of the initial $\phi_1 \pi$ and ϕ_1 candidate reconstructions, respectively.

The presence of a second distinct $D_s^{(*)}$ candidate was determined by searching for a different $K^+ K^-$ candidate system representing the ϕ_2 component, similarly selected but required to share a vertex with the muon candidate, which is taken by definition as a daughter of the second $D_s^{(*)}$ candidate. A two-dimensional unbinned likelihood fit was used to identify the correlation between the $\phi_1 \pi$ and ϕ_2 candidates, yielding 31.0 ± 9.4(stat.) $\phi_2 \mu$ candidates with a statistical significance of 3.7 standard deviations. Figs. 6 and 7 illustrate the result of modifying Fig. 4 with the ϕ_2 candidate requirement and the inclusive ϕ_2 invariant mass distribution, respectively. The resultant branching-fraction measurement is extracted by normalizing to the reference mode $B_s^0 \to D_s^{(*)} \mu \nu$, the branching fraction for which contributes the largest systematic uncertainty to the result; the absolute $B_s^0 \to D_s^{(*)} D_s^{(*)}$ branching fraction is summarized in Sect. 3.3 below.

3.2. CDF Exclusive $\mathcal{B}(B_s^0 \to D_s^- D_s^+)$

The first observation of the exclusive decay $B_s^0 \to D_s^- D_s^+$ was made by the CDF Collaboration in 355 pb^{-1} of $p\bar{p}$ collisions at $\sqrt{s} = 1.96$ TeV [9]. The $B_s^0 \to D_s^- D_s^+$ mode is deemed to be purely CP even due to quark-level effects, meaning that the B_s^0 parent is essentially always the light mass eigenstate in this case. The experimental approach used was to reconstruct candidates exclusively by combining three dif-

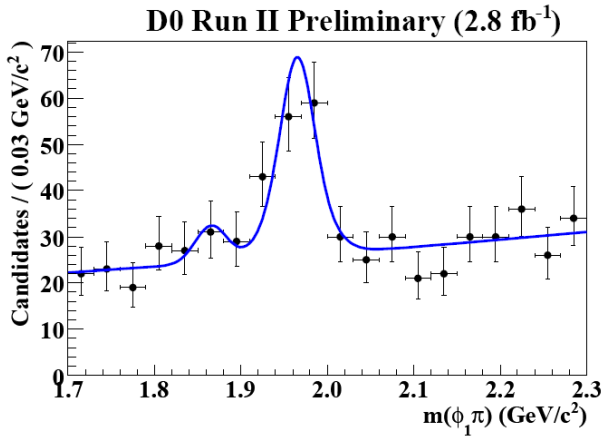

Figure 6: Inclusive $D^{(*)}$ candidate reconstruction in the μ sample with the additional $\phi_2\,\mu$ requirement applied, represented by the $\phi_1\,\pi$ invariant mass distribution corresponding to the $K^+\,K^-$ signal region, $1.01 < m(K^+\,K^-) < 1.03$ GeV/c^2 [8]. The two peaks represent the observed $D^{\pm}$ and $D_s^{\pm}$ inclusive candidate yields.

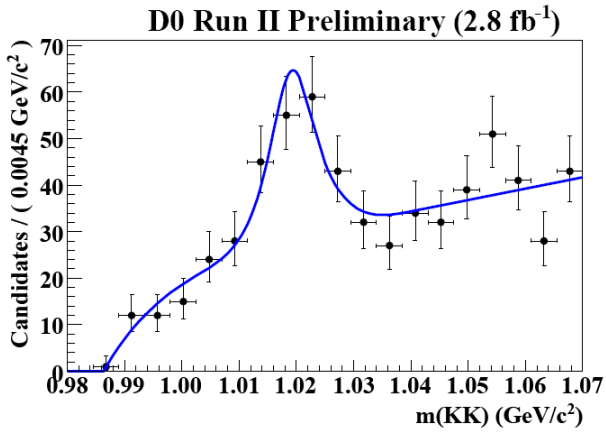

Figure 7: Inclusive $K^+\,K^-$ invariant mass distribution for ϕ_2 candidates composed of tracks other than those used to form ϕ_1 candidates [8].

ferent D_s^+ meson decay modes to the $\phi\,\pi^+$, $\bar{K}^{*0}\,K^+$, and $\pi^+\,\pi^+\,\pi^-$ final states for one of the B_s^0 candidate daughters while reconstructing the second daughter solely using the $\phi\,\pi^-$ mode. Analogous $B^0 \to D^-\,D_s^+$ decay candidates, with $D^- \to K^+\,\pi^-\,\pi^-$, were reconstructed in parallel for normalization purposes, with an attendant cancellation of several systematic uncertainties.

Strong signals with well understood backgrounds were reconstructed for all three of the reference $B^0 \to D^-\,D_s^+$ decay modes [9]. Fig. 8 depicts the invariant mass distributions and signal fits for the three $B_s^0 \to D_s^-\,D_s^+$ decay channels. The individual significances of the signal reconstructed with the modes containing the $D_s^+ \to \phi\,\pi^+$, $D_s^+ \to \bar{K}^{*0}\,K^+$, and $D_s^+ \to \pi^+\,\pi^+\,\pi^-$ final states were found to be 5.8, 3.4, and 4.4 standard deviations, respectively. The product of the three likelihoods was used to find a combined result consistent with an observation of $B_s^0 \to D_s^-\,D_s^+$ decay with 7.5 standard deviations of significance. After correcting the relative event yields for relative acceptances and efficiencies, the ratio of branching fractions was measured to be $\mathcal{B}(B_s^0 \to D_s^-\,D_s^+)/\mathcal{B}(B^0 \to D^-\,D_s^+) = 1.44^{+0.48}_{-0.44}$, where world-average measurements [10] were employed to correct for the relative fragmentation fractions f_d/f_s and daughter branching fractions $\mathcal{B}(D^- \to K^+\,\pi^-\,\pi^-)/\mathcal{B}(D_s^- \to \phi\,\pi^-)$, both of which contribute prominently to the total systematic uncertainty of the measurement.

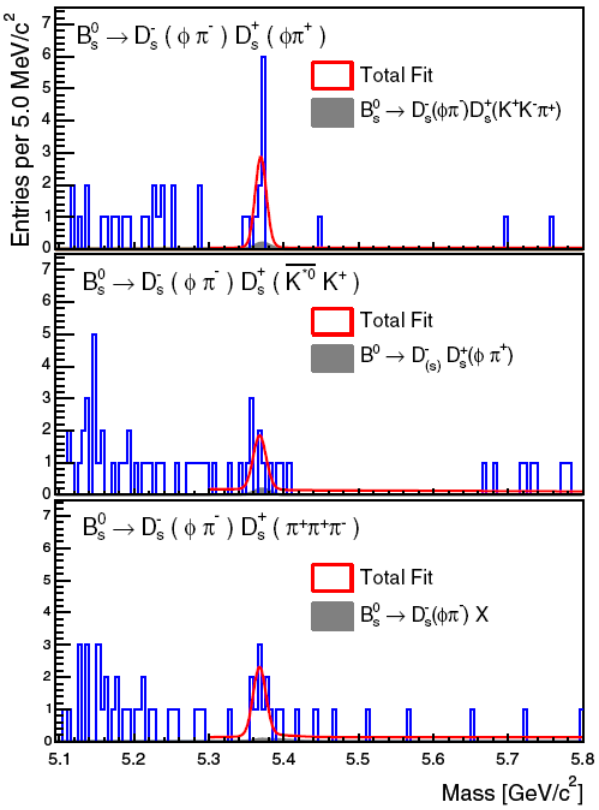

Figure 8: Invariant mass distributions for $B_s^0 \to D_s^-\,D_s^+$ candidates (histogram), where $D_s^+ \to \phi\,\pi^+$ (top), $D_s^+ \to \bar{K}^{*0}\,K^+$ (middle), and $D_s^+ \to \pi^+\,\pi^+\,\pi^-$ (bottom) [9]. The red curves describe the total fit result whereas the grey shaded regions represent the principal background component in each case.

3.3. Absolute $B_s^0 \to D_s^{(*)}\,D_s^{(*)}$ Branching Fractions: Worldwide Status

The 3.7 standard deviation DZero measurement [8] described in Sect. 3.1 above yielded an absolute branching fraction $\mathcal{B}(B_s^0 \to D_s^{(*)}\,D_s^{(*)}) = 0.042 \pm 0.015(\text{stat.}) \pm 0.017(\text{syst.})$, which confirms and is significantly more precise than the PDG-updated [10]

measurement of the first observation by ALEPH [11], $0.12 \pm 0.05(\text{stat.})\ ^{+0.10}_{-0.04}(\text{syst.})$.

The 7.5 standard deviation CDF measurement [9] described in Sect. 3.2 above yielded an absolute branching fraction $\mathcal{B}(B_s^0 \to D_s^- D_s^+) = \left(9.4^{+4.4}_{-4.2}\right) \times 10^{-3}$, representing the first observation of this mode.

The Belle collaboration has also recently placed limits on the three exclusive decay constituents of the $B_s^0 \to D_s^{(*)} D_s^{(*)}$ system of modes. The results, which are based on a 1.86 fb^{-1} data sample obtained at the $\Upsilon(5S)$ resonance in e^+e^- collisions at the KEKB asymmetric collider, are $\mathcal{B}(B_s^0 \to D_s^- D_s^+) < 6.7\%$, $\mathcal{B}(B_s^0 \to D_s^{*+} D_s^-) < 12.1\%$, and $\mathcal{B}(B_s^0 \to D_s^{*+} D_s^{*-}) < 25.7\%$, each at 90% confidence level [12].

By invoking certain theoretical assumptions, measurements of $\mathcal{B}(B_s^0 \to D_s^{(*)} D_s^{(*)})$ and $\mathcal{B}(B_s^0 \to D_s^- D_s^+)$ can readily be applied to estimating or placing a lower bound on $\Delta\Gamma_s^{CP}/\Gamma_s$, as discussed at the beginning of Sect. 3. Both the DZero and CDF branching-fraction measurements suggest values of $\Delta\Gamma_s^{CP}/\Gamma_s$ consistent with the Standard Model, which assumes negligible CP violation in B_s^0 mixing.

4. First $B_s^0 \to D_{s1}^-(2536)\mu^+\nu X$ Observation

A significant fraction of B_s^0 mesons decay semileptonically to orbitally excited P-wave D_s^{**} mesons. Measurements of such exclusive semileptonic branching fractions are useful for comparisons of inclusive and exclusive decay rates, the extraction of CKM matrix elements, B_s^0 mixing analyses, and studies of theoretical hadronic form-factor models. The DZero collaboration recently made the first observation of the decay $B_s^0 \to D_{s1}^-(2536)\,\mu^+\,\nu_\mu\,X$ in 1.3 fb^{-1} of $p\bar{p}$ collisions at $\sqrt{s} = 1.96$ TeV [13].

Based on a sizeable sample of $87\,506 \pm 496(\text{stat.})$ D^* meson candidates in an inclusive muon dataset, candidate $D^*\,K_S$ invariant mass combinations were constructed as illustrated in Fig. 9. The indicated fit determined a $D_{s1}(2536)$ yield of $45.9 \pm 9.1(\text{stat.})$ candidates with a statistical significance of 6.1 standard deviations, and a mass of the $D_{s1}(2536)$ candidate of $2535.7 \pm 0.6(\text{stat.}) \pm 0.5(\text{syst.})$ MeV/c^2, which was consistent with the PDG world-average value [10]. Assuming that $D_{s1}^-(2536)$ production in semileptonic decays arises solely from B_s^0 meson decays, the DZero collaboration measured the following product of fragmentation and branching fractions: $f_s \cdot \mathcal{B}(B_s^0 \to D_{s1}^-(2536)\,\mu^+\,\nu_\mu\,X) \cdot \mathcal{B}(D_{s1}^-(2536) \to D^{*-}\,K_S) = [2.66 \pm 0.52(\text{stat.}) \pm 0.45(\text{syst.})] \times 10^{-4}$. The derivation of an absolute $\mathcal{B}(B_s^0 \to D_{s1}^-(2536)\,\mu^+\,\nu_\mu\,X)$ branching fraction from this measured product is useful for comparisons with theoretical calculations, but requires an assumption for the $D_{s1}(2536)$ daughter branching fraction and is degraded by the sizeable world-average experimental uncertainty on f_s [10].

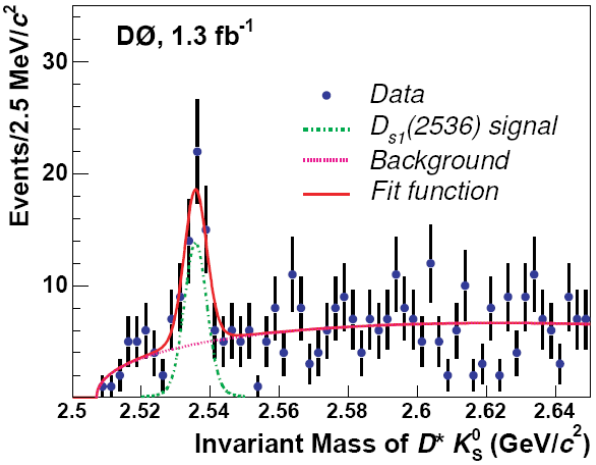

Figure 9: Invariant mass distribution of $D^*\,K_S$ candidates with an associated muon candidate [13]. The result of the fit to the signal and background is shown by the curves.

5. Recent B_s^0 Radiative Decay Results

One-loop effective flavour-changing neutral-current radiative penguin decays are well known as possible venues for new physics beyond the Standard Model. Hitherto unobserved particles can first reveal their existence in the virtual loop propagator by modifying the Standard Model couplings, and hence decay rates, in measurable ways. In the following, studies of two radiative penguin B_s^0 decay modes conducted by the Belle collaboration using 23.6 fb^{-1} of asymmetric e^+e^- $\Upsilon(5S)$ collision data [14] are reviewed.

5.1. First $B_s^0 \to \phi\,\gamma$ Observation

The decay $B_s^0 \to \phi\,\gamma$ is described by the Standard Model using a one-loop radiative penguin diagram, as indicated in Fig. 10. The mode may be considered to be the strange analogue of the $B \to K^*(892)\,\gamma$ decays, which provided the first explicit observation of penguin processes [15]. The subsequent observed agreement between numerous experimental results for $b \to s\,\gamma$ rates and Standard Model expectations provides a strong theoretical constraint also for the analogous $B_s^0 \to \phi\,\gamma$ decay discussed here.

The Belle analysis [14] made use of a three-dimensional unbinned maximum likelihood fit involving observables of beam-energy-constrained mass $M_{\rm bc}$, energy difference ΔE, and the cosine of the helicity angle $\cos\theta_{\rm hel}$, where $\theta_{\rm hel}$ was the angle between the B_s^0 and K^+ mesons in the ϕ meson rest frame. Projections on to these three observables and the fit results are illustrated in Figs. 11, 12, and 13.

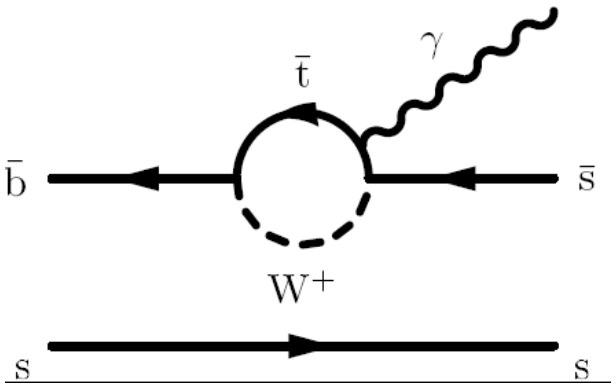

Figure 10: Diagrammatic representation of the most probable decay process for the $B_s^0 \to \phi\,\gamma$ mode [14].

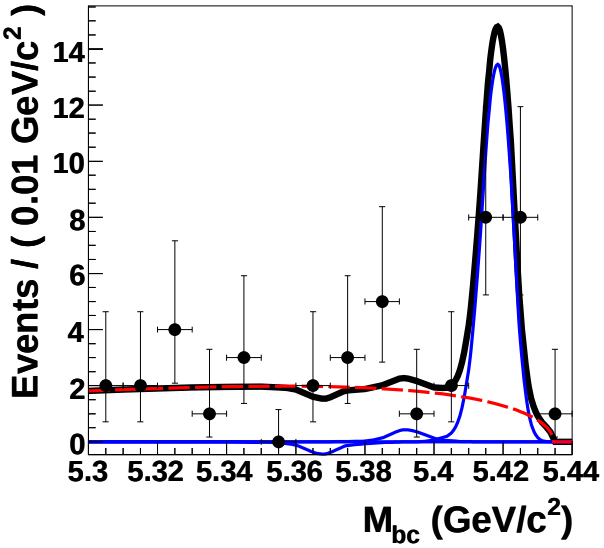

Figure 11: The beam-energy-constrained mass $M_{\rm bc}$ projection and fit results [14]. The points represent data, the thick (black) solid curve is the fit function, the thin (blue) curve is the signal function, and the dashed (red) curve represents the continuum contribution.

The fit resulted in 18^{+6}_{-5} signal candidates with a statistical significance of 5.5 standard deviations, and a first observed branching fraction of $\mathcal{B}(B_s^0 \to \phi\,\gamma) = \left[57\,^{+18}_{-15}(\text{stat.})\,^{+12}_{-11}(\text{syst.})\right] \times 10^{-6}$ was determined [14].

5.2. Search for Radiative $B_s^0 \to \gamma\,\gamma$ Decay

As for the $B_s^0 \to \phi\,\gamma$ mode, the $B_s^0 \to \gamma\,\gamma$ channel, a diagram for which is depicted in Fig. 14, is similarly expected to be largely constrained by the known $B \to X_s\,\gamma$ branching fraction [16]; however, various new physics sources have been suggested that could enhance the $B_s^0 \to \gamma\,\gamma$ branching fraction by up to an order of magnitude without compromising this constraint. These include a two Higgs doublet model with

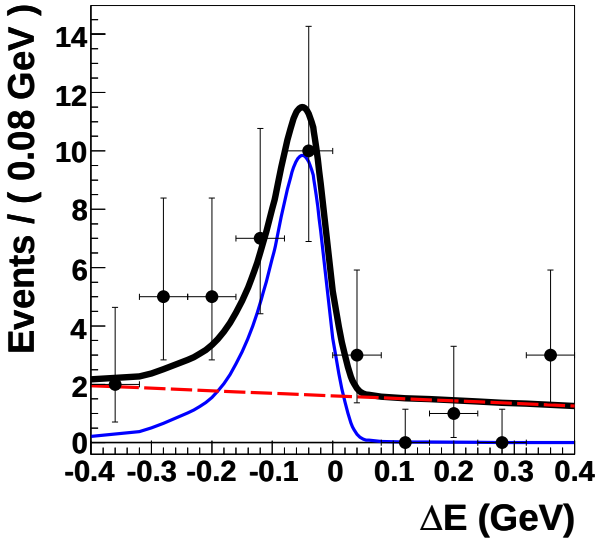

Figure 12: The energy difference ΔE projection and fit results [14]. The curves and markers are as described in Fig. 11.

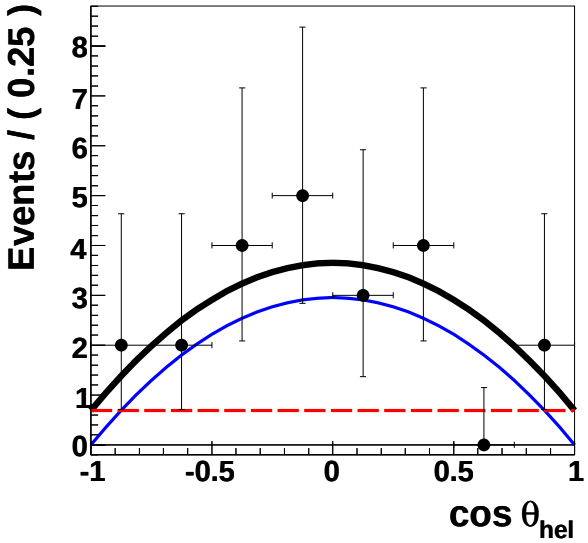

Figure 13: The $\cos\theta_{\rm hel}$ projection and fit results [14]. The curves and markers are as described in Fig. 11.

flavour-changing neutral currents [17], a fourth-quark generation [18], and supersymmetry with broken R-parity [19].

The Belle $B_s^0 \to \gamma\,\gamma$ analysis consisted of a two-dimensional unbinned maximum likelihood fit involving the $M_{\rm bc}$ and ΔE observables previously defined in Sect. 5.1. Figs. 15 and 16 depict the projections on to the two observables as well as the fit results.

There being no significant $B_s^0 \to \gamma\,\gamma$ signal observed, the Belle collaboration set a 90% confidence level branching-fraction limit of $\mathcal{B}(B_s^0 \to \gamma\,\gamma) <$

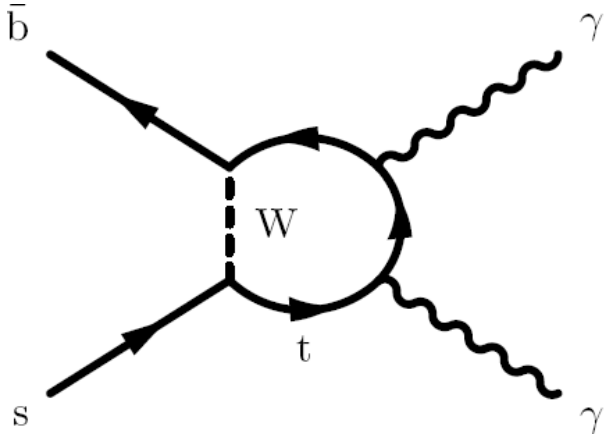

Figure 14: Diagrammatic representation of the most probable decay process for the $B_s^0 \to \gamma\,\gamma$ mode [14] .

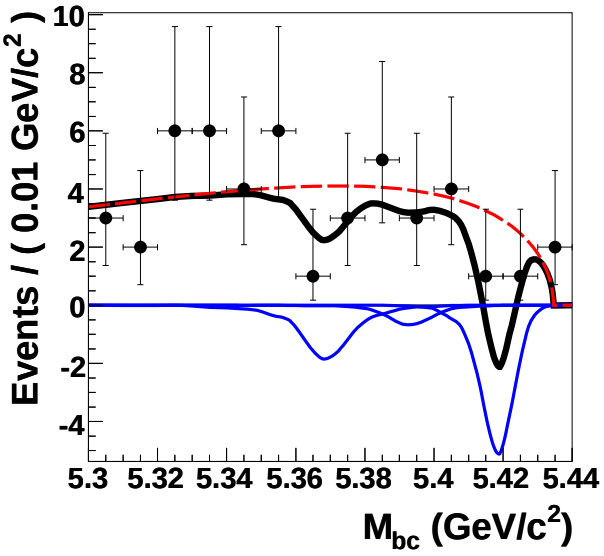

Figure 15: The beam-energy-constrained mass $M_{\rm bc}$ projection and fit results [14]. The points represent data, the thick (black) solid curve is the fit function, the thin (blue) curve is the signal function, and the dashed (red) curve represents the continuum contribution.

8.7×10^{-6}, which, though six times more restrictive than the previous limit [12], still stands at least an order of magnitude higher than the Standard Model and new physics predictions.

6. Charmless Two-Body B_s^0 Modes

Two-body charmless hadronic decays of neutral b hadrons can provide insight into both the CKM matrix and possible new physics phenomena. The CDF experiment can reconstruct significant samples of these decay modes by virtue of the high yields of b-quark production at the Fermilab Tevatron $p\bar{p}$ collider

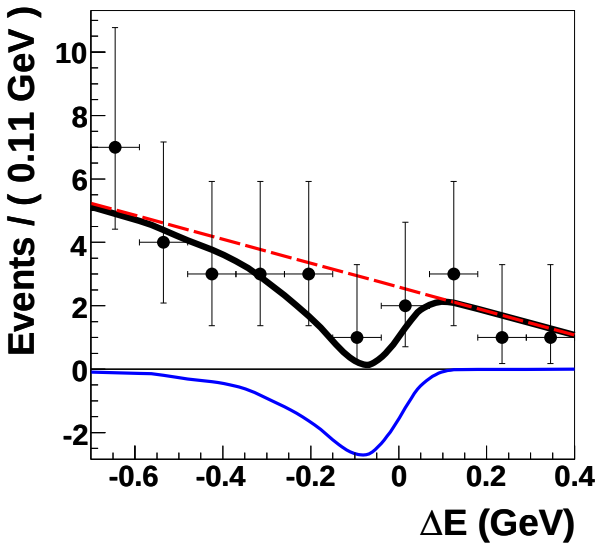

Figure 16: The energy difference ΔE projection and fit results [14]. The curves and markers are as described in Fig. 15.

and the use of a dedicated trigger on impact parameters of charged-particle tracks, discussed in Sect. 2.

The degree of penguin-tree interference at play in these decay modes depends on the CKM angle γ (ϕ_3), hadronic amplitudes and phases, and possibly the presence of new physics. Strategies for understanding this fertile system of processes involve the study of several modes related by isospin and $SU(3)$ flavour and the combination of multiple observables such as branching fractions and CP asymmetries.

The CDF collaboration recently updated its suite of $B_{(s)}^0 \to h^+ h'^-$ branching-fraction results based on 1 fb^{-1} of $p\bar{p}$ collisions at $\sqrt{s} = 1.96$ TeV [20], where h denotes either a π or K meson. The main change, which consisted of a better determination of the relative isolation efficiencies for B^0 and B_s^0 candidates, resulted in improved branching-fraction measurements for the B_s^0 modes. The results, for which the largest systematic uncertainties arose due to dE/dx particle-identification aspects, are summarized in Table I and compared with a set of theoretical predictions [22], which shows good agreement. Another more recent set of predictions due to Chiang and Zhou [23] also shows reasonable agreement. More theoretical calculations are cited in Ref. [24].

For meaningful comparisons of experiment and theory, however, it is important that the scope be widened to include also the B^+ and B^0 branching fractions, as well as the CP asymmetries. Inconsistencies between the current landscape of experimental results and theoretical predictions suggest that there may be more $SU(3)$ breaking than expected in the strong phases or that there has been a breakdown of QCD factorization [25].

Table I Updated $B_s^0 \to h^+ h'^-$ signal yields, ratios of product fragmentation and branching-fraction measurement results, and derived absolute branching-fraction results from CDF [20] with input from the HFAG [21]. Where applicable, the first uncertainties are statistical and the second are systematic. The rightmost column represents an example theoretical prediction by Beneke and Neubert [22] for comparison with the measured results. The ranges shown for the theoretical prediction represent coverage of multiple theory parameter fit scenarios; theoretical uncertainties are not indicated.

Decay Mode	**Signal Yield**	**CDF Measurement [20]**	$\mathcal{B} \times 10^6$ **CDF Derived**	$\mathcal{B} \times 10^6$ **Beneke & Neubert [22]**
$B_s^0 \to K^+ K^-$	1307 ± 64	$\frac{f_s}{f_d} \cdot \frac{\mathcal{B}(B_s^0 \to K^+ K^-)}{\mathcal{B}(B^0 \to K^+ \pi^-)} = 0.347 \pm 0.020 \pm 0.021$	$25.8 \pm 1.5 \pm 3.9$	$28 \to 36$
$B_s^0 \to K^- \pi^+$	$230 \pm 34 \pm 16$	$\frac{f_s}{f_d} \cdot \frac{\mathcal{B}(B_s^0 \to K^- \pi^+)}{\mathcal{B}(B^0 \to K^+ \pi^-)} = 0.071 \pm 0.010 \pm 0.007$	$5.27 \pm 0.74 \pm 0.90$	$6.8 \to 10.4$
$B_s^0 \to \pi^+ \pi^-$	$26 \pm 16 \pm 14$	$\frac{f_s}{f_d} \cdot \frac{\mathcal{B}(B_s^0 \to \pi^+ \pi^-)}{\mathcal{B}(B^0 \to K^+ \pi^-)} = 0.007 \pm 0.004 \pm 0.005$	< 1.3 @ 90% CL	$0.027 \to 0.155$

7. First $\Lambda_b^0 \to p\,(\pi^-, K^-)$ Observations

No CP-violating decay-rate asymmetries have previously been measured in baryon decays. Two-body charmless decays of Λ_b^0 baryons with a final-state proton and a charged pion or kaon are self tagging and therefore promising vehicles for the study of CP-violating asymmetries [26]. CDF is currently the only experiment able to collect and reconstruct such two-body b-baryon decay candidates [27].

Branching fractions of $\Lambda_b^0 \to p\,\pi^-$ and $\Lambda_b^0 \to p\,K^-$ decays have also been shown to have possible sensitivity to new physics. Mohanta has provided a prediction suggesting that Minimal Supersymmetric Extensions of the Standard Model in which R-parity is violated could enhance these branching fractions by a factor of $\mathcal{O}(100)$ [28].

The analysis approach employs the same trigger and fit machinery as that used to obtain the results reported in Sect. 6 above, but has been optimized specifically for dedicated measurements of $\Lambda_b^0 \to p\,\pi^-$ and $\Lambda_b^0 \to p\,K^-$ branching fractions (and CP asymmetries, though these lie beyond the scope of this review). Details of the candidate selection criteria are provided in Ref. [27]. A fit is performed in terms of a particle-identification observable and three kinematic variables: an invariant mass calculated with a pion hypothesis assigned to both charged tracks; a signed momentum imbalance $\alpha \equiv (1 - p_1/p_2)q_1$, where p_1 (p_2) is the lower (higher) of the particle momenta and q_1 is the sign of the charge of the track with momentum p_1; and the scalar sum of the two track momenta. A projection of the dipion invariant mass observable and the fit results is illustrated in Fig. 17.

The signal yields were corrected for efficiencies and related to the abundant $B^0 \to K^+\pi^-$ mode, whose branching fraction is known with B-factory precision [10]. The preliminary observed branching-fraction ratios, measured in a product with the ratios of production cross sections and fragmentation fractions, were [27]

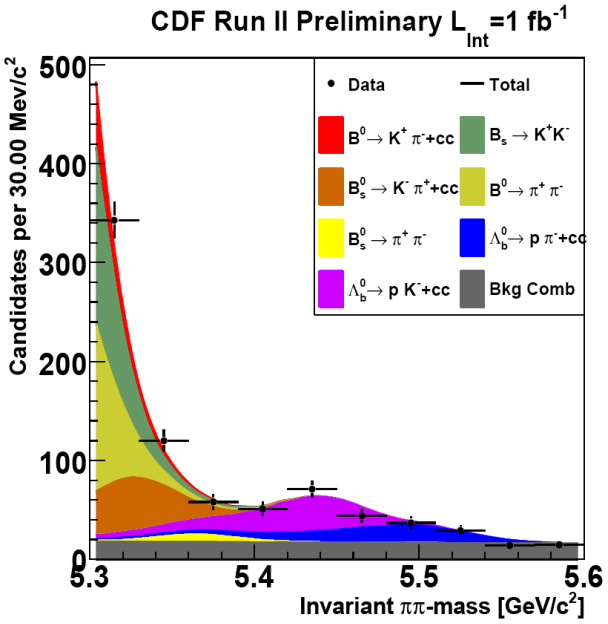

Figure 17: The dipion invariant mass $M_{\pi\pi}$ projection and fit results [27]. The signal $\Lambda_b^0 \to p\,\pi^-$ and $\Lambda_b^0 \to p\,K^-$ contributions are indicated in blue and magenta, respectively.

$$\frac{\sigma(p\bar{p} \to \Lambda_b^0 X, p_T > 6\,\mathrm{GeV}/c)}{\sigma(p\bar{p} \to B^0 X, p_T > 6\,\mathrm{GeV}/c)} \frac{\mathcal{B}(\Lambda_b^0 \to p\,\pi^-)}{\mathcal{B}(B^0 \to K^+\pi^-)} = 0.0415 \pm 0.0074(\mathrm{stat.}) \pm 0.0058(\mathrm{syst.})$$

and

$$\frac{\sigma(p\bar{p} \to \Lambda_b^0 X, p_T > 6\,\mathrm{GeV}/c)}{\sigma(p\bar{p} \to B^0 X, p_T > 6\,\mathrm{GeV}/c)} \frac{\mathcal{B}(\Lambda_b^0 \to p\,K^-)}{\mathcal{B}(B^0 \to K^+\pi^-)} = 0.0663 \pm 0.0089(\mathrm{stat.}) \pm 0.0084(\mathrm{syst.}),$$

for which the candidate isolation efficiencies constituted the dominant source of systematic uncertainty. Preliminary measurements of the CP decay-rate asymmetries for the $\Lambda_b^0 \to p\,\pi^-$ and $\Lambda_b^0 \to$

$p K^-$ modes were also computed and are reported in Ref. [27].

World-average values of the poorly known ratio of fragmentation fractions $f_{b-\mathrm{baryon}}/f_d$ and the $B^0 \to K^+\pi^-$ decay rate [10] were used to extract the derived absolute branching fractions [27]

$$\mathcal{B}(\Lambda_b^0 \to p\pi^-) = [3.1 \pm 0.6(\mathrm{stat.}) \pm 0.7(\mathrm{syst.})] \times 10^{-6}$$

and

$$\mathcal{B}(\Lambda_b^0 \to pK^-) = [5.0 \pm 0.7(\mathrm{stat.}) \pm 1.0(\mathrm{syst.})] \times 10^{-6},$$

which agree with Standard Model expectations and exclude the $\mathcal{O}(10^{-4})$ branching fractions predicted by the R-parity violating Minimal Supersymmetric extension of the Standard Model [28].

8. Conclusions

Recent studies of $p\bar{p}$ and e^+e^- collisions by the Belle, CDF, and DZero collaborations have yielded a plethora of new decay observations and branching-fraction measurements for B_s^0 mesons and Λ_b^0 baryons. First observations and new results in three classes of $B_s^0 \to D_s^{(*(*))}X$ modes have recently been reported; the first radiative penguin in the B_s^0 system, $B_s^0 \to \phi\gamma$, has been observed and the branching fraction measured; a significantly reduced upper limit has been determined for the radiative $B_s^0 \to \gamma\gamma$ mode, which has been deemed sensitive to a number of possible new physics scenarios; $B_s^0 \to h^- h'^+$ decay rates, which are crucial to the formation of a consistent picture between experiment and theory in the larger space of two-body charmless b-hadron decay rates and CP asymmetries, have been updated; and first observations of the modes $\Lambda_b^0 \to p\pi^-$ and $\Lambda_b^0 \to pK^-$ have been made and their branching fractions preliminarily measured.

A recurring aspect in the study of B_s^0 and b-baryon decay rates at $p\bar{p}$ and e^+e^- colliders is the reliance on $f_s(b \to B_s^0)$ and $f_{b-\mathrm{baryon}}(b \to \Lambda_b^0)$ fragmentation fractions for interpretation of the results. These fragmentation fractions, in particular their dependence on the b-quark momentum and the accelerator collision environment, are poorly understood and have so far been measured with sizeable uncertainties [10]. Improved measurements of f_s and $f_{b-\mathrm{baryon}}$ are therefore crucial to this important heavy b-hadron frontier of flavour physics.

Given the recent results, further study with additional data is strongly warranted to hunt for signs of new physics lying beyond the Standard Model, to seek answers to theoretical questions about Standard-Model manifestations of electroweak and QCD phenomenology, to employ flavour-tagging techniques, and to continue exploration of this rich and exciting sector of flavour particle physics. Further to the results presented in this review, an additional $2-3\times$ factor of time-integrated luminosity is expected to be analyzed from the Fermilab Tevatron, the LHCb experiment is expected to begin datataking soon at CERN, and a high-intensity Super-B facility is envisaged in the coming years.

Acknowledgments

Colleagues in the Belle, CDF, and DZero collaborations, as well as the numerous technical and accelerator personnel at Fermilab and KEK, are acknowledged for their vital contributions to the results described in this review. The FPCP 2008 organizers are also warmly thanked for arranging an enjoyable and stimulating meeting at the National Taiwan University in Taipei.

References

1 R. Aleksan, I. Dunietz, and B. Kayser, Z. Phys. C **54**, 653 (1992).
2 I. Dunietz, Phys. Rev. D **52**, 3048 (1995), arXiv:hep-ph/9501287.
3 CDF Collaboration, CDF Public Note 8850, to be submitted to Phys. Rev. Lett, available at `http://www-cdf.fnal.gov/physics/new/bottom/070524.blessed-Bs-DsK/cdf8850.pdf`.
4 W. Ashmanskas *et al.*, Nucl. Instrum. Meth. A **518**, 532 (2004), arXiv:physics/0306169.
5 A. Abulencia *et al.* [CDF Collaboration], Phys. Rev. Lett. **98**, 061802 (2007), arXiv:hep-ex/0610045.
6 A. Abulencia *et al.* [CDF Collaboration], Phys. Rev. Lett. **97**, 242003 (2006), arXiv:hep-ex/0609040.
7 Y. Grossman, Phys. Lett. B **380**, 99 (1996), arXiv:hep-ph/9603244; I. Dunietz, R. Fleischer, and U. Nierste, Phys. Rev. D **63**, 114015 (2001), arXiv:hep-ph/0012219.
8 DZero Collaboration, DZero Public Note 5651-CONF (May 2, 2008), available at `http://www-d0.fnal.gov/Run2Physics/WWW/results/prelim/B/B53/B53.pdf`
9 T. Aaltonen *et al.* [CDF Collaboration], Phys. Rev. Lett. **100**, 021803 (2008).
10 W.-M. Yao *et al.* [Particle Data Group], J. Phys. G **33**, 1 (2006) and web update (2007): `http://pdg.lbl.gov`.
11 R. Barate *et al.* [ALEPH Collaboration], Phys. Lett. B **486**, 286 (2000).
12 A. Drutskoy *et al.* [Belle Collaboration], Phys. Rev. D **76**, 012002 (2007), arXiv:hep-ex/0610003v4.

13 V.M. Abazov *et al.* [DZero Collaboration], arXiv:0712.3789 [hep-ex], submitted to Phys. Rev. Lett.

14 J. Wicht *et al.* [Belle Collaboration], Phys. Rev. Lett. **100**, 121801 (2008), arXiv:0712.2659 [hep-ex].

15 R. Ammar *et al.* [CLEO Collaboration], Phys. Rev. Lett. **71**, 674 (1993).

16 S. Bertolini and J. Matias, Phys. Rev. D **57**, 4197 (1998), arXiv:hep-ph/9709330.

17 T.M. Aliev and E.O. Iltan, Phys. Rev. D **58**, 095014 (1998), arXiv:hep-ph/9803459.

18 W.J. Huo, C.D. Lu, and Z.J. Xiao, arXiv:hep-ph/0302177.

19 A. Gemintern, S. Bar-Shalom, and G. Eilam, Phys. Rev. D **70**, 035008 (2004), arXiv:hep-ph/0404152.

20 CDF Collaboration, CDF Public Note 8579v1 (updated Apr. 10, 2008), available at `http://www-cdf.fnal.gov/physics/new/bottom/060921.blessed-bhh_1fb/public_note/cdf8579_bhh_1fb_public_v1.ps`

21 E. Barberio *et al.* [Heavy Flavour Averaging Group (HFAG)], arXiv:0704.3575 [hep-ex].

22 M. Beneke and M. Neubert, Nucl. Phys. **B675**, 333 (2003), arXiv:hep-ph/0308039.

23 C.-W. Chiang and Y.-F. Zhou, JHEP**0612**, 027 (2006), arXiv:hep-ph/0609128.

24 A. Abulencia *et al.* [CDF Collaboration], Phys. Rev. Lett. **97**, 211802 (2006), arXiv:hep-ex/0607021.

25 C.-W. Chiang, M. Gronau, and J.L. Rosner, arXiv:0803.3229v3 [hep-ph], submitted to Phys. Lett. B.

26 R. Mohanta, A.K. Giri, and M.P. Khanna, Phys. Rev. D **63**, 074001 (2001), arXiv:hep-ph/0006109.

27 CDF Collaboration, CDF Public Note 9092 (updated Jan. 9, 2008), available at `http://www-cdf.fnal.gov/physics/new/bottom/071018.blessed-ACP_Lambdab_ph/cdf9092_public_Lbph_CP-BR.ps`

28 R. Mohanta, Phys. Rev. D **63**, 056006 (2001), arXiv:hep-ph/0005240.